Astronomical and Astrophysical Transactions (*AApTr*), 2022, Vol. 33, Issue 3, pp. 191–204,
ISSN 1055-6796, Photocopying permitted by license only, ©Cambridge Scientific Publishers

On the nature of the ultrarelativistic prompt emission phase of GRB 190114C and GRB 180720B

R. Ruffini[1,2,*] | in collaboration with Y. Aimuratov, L.M. Becerra, C.L. Bianco, S. Campion, Y.C. Chen, C. Cherubini, S. Filippi, M. Karlica, L. Li, G.J. Mathews, R. Moradi, M. Muccino, G.B. Pisani, J.A. Rueda, N. Sahakyan, Y. Wang, S.S. Xue

[1] *ICRANet, Piazza della Repubblica 10, I-65122 Pescara, Italy*
[2] *INAF, Viale del Parco Mellini 84, 00136 Roma, Italy*

Received 14 December, 2022

A profound difference has occurred in the analysis of GRBs initially analyzed in the domain of gamma-ray astronomy with the Compton Gamma Ray Observatory and the BATSE Detector with the extension to X-ray astronomy and optical astronomy introduced by Beppo-SAX and the KEK and VLT optical observatory, followed by the AGILE, Fermi mission, Niels Gehrels SWIFT mission as well as HEHSS and MAGIC observations. An authentic "Copernican revolution" has occurred in the transition from the traditional model of GRBs originating in a single star progenitor (collapsar) to GRBs with a binary progenitor composed of a CO core and a companion NS. We evidence from 24 SN observations related to GRBs that all of them, once analyzed with the general relativistic corrections, can be identified with I Bc Sn with a common value of the luminosity and common time of occurrence of the peak of the optical emission. This can be understood in terms of a precursor composed of a CO core and a binary NS companion. By contrast, the GRBs differ profoundly in their energetics which can be expressed in terms of 3 different classes of BDHNe: BDHN I, BDHN II, BDHN III, also originating from precursors composed of a CO core and a binary companion. It is pointed out how the analysis of these systems has profoundly modified the concept of the BH and the associated fundamental physics necessary for their description since the publication of "Introducing the Black Hole" by Ruffini and Wheeler in 1971. At first, it is illustrated how the most radical change has occurred in the introduction of the effective BH charge, with an electric field only function of the BH dimensionless spin and a background magnetic field B_0. This definitely indicates the abandonment of the Kerr–Newman solution in favour of the Kerr metric, for energy extraction processes in BH physics. We then enter in the detailed description of the "seven Seals", the seven Episodes characterizing GRB 190114c and the associated SN 2019jrj.

Based on the article by Aimuratov et al., in preparation.

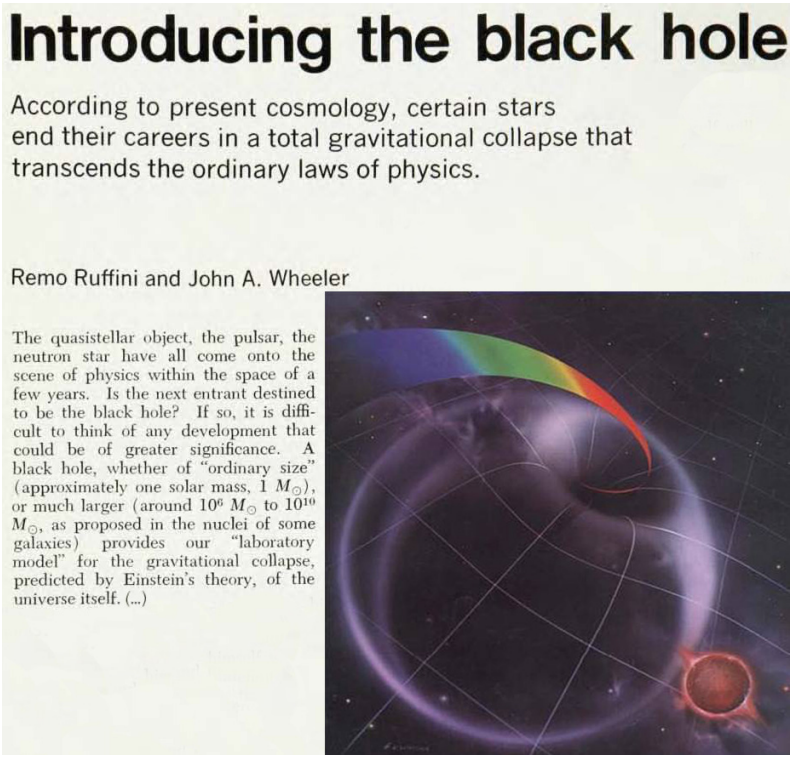
Keywords: Black hole, supernova, hypernova, binary driven hypernova

*Email: ruffini@icra.it

1 Introducing the Black Hole

In the 1971 article, Ruffini and Wheeler, "Introducing the Black Hole" (Ruffini & Wheeler, 1971), the structure underlying this new astrophysical object was identified:

1. in the Kerr metric. This formula had emerged from the mathematical work of Aleksei Petrov at Kazan University and brought to its final form by Roy Kerr at the University of Texas in Austin. The earliest physical implementation of the structure of the BH was based on two approaches:
2. the descriptions of free massive particles moving in the Kerr metric by Carter, Ruffini and Wheeler (1969), quoted in Vol. 2 of Landau & Lifshitz (1975);
3. on the Mass Energy formula of the Kerr Metric, Christodoulou, Phys. Rev. Lett., 25 (1970) 1596 (received September 17, 1970) (Christodoulou, 1970), extended to the presence of charge by Christodoulou and Ruffini (1970), Phys. Rev. D, 4 (1971) 3552 (received March 1, 1971), followed ten days after by Stephen Hawking, Phys. Rev. Lett., 26 (1971) 1344 (received March 11, 1971) (Hawking, 1971) and Commun. Math. Phys., 25 (1972) 152 (received October 15, 1971) (Hawking, 1972).



Introducing the black hole

According to present cosmology, certain stars end their careers in a total gravitational collapse that transcends the ordinary laws of physics.

Remo Ruffini and John A. Wheeler

The quasistellar object, the pulsar, the neutron star have all come onto the scene of physics within the space of a few years. Is the next entrant destined to be the black hole? If so, it is difficult to think of any development that could be of greater significance. A black hole, whether of "ordinary size" (approximately one solar mass, 1 $M_\odot$), or much larger (around 10^6 $M_\odot$ to 10^{10} $M_\odot$, as proposed in the nuclei of some galaxies) provides our "laboratory model" for the gravitational collapse, predicted by Einstein's theory, of the universe itself. (...)

Figure 1 From "Introducing the Black Hole" (Ruffini & Wheeler, 1971), Physics Today 24, 1, 30.

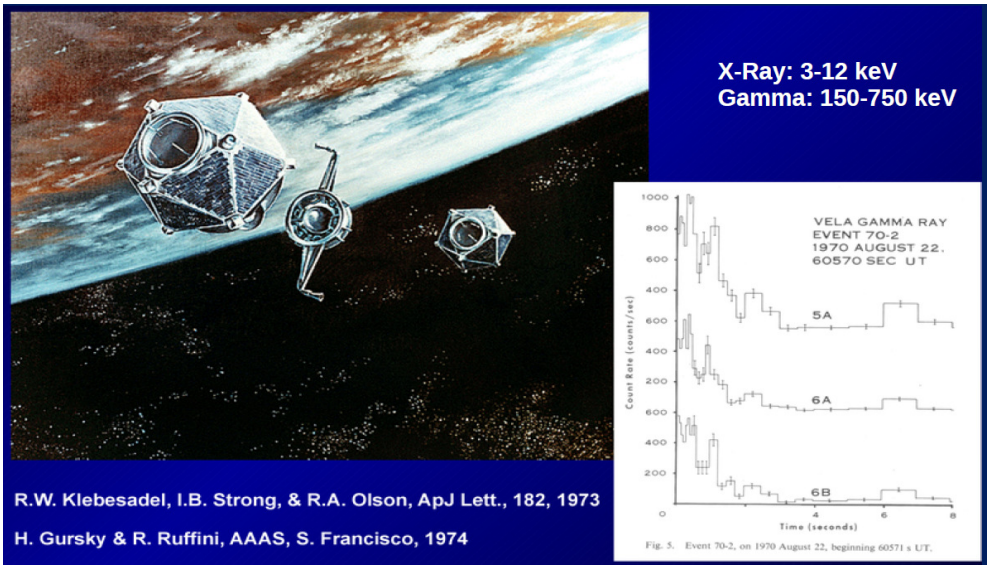


Figure 2 Vela satellites and GRBs (60s–70s). From R.W. Klebesadel, I.B. Strong, R.A. Olson, ApJ Lett., 182, 1973 (Klebesadel, Strong, & Olson, 1973) and Gursky & Ruffini (1975).

$$m^2 = \left(m_{ir} + \frac{e^2}{4m_{ir}}\right) + \frac{L^2}{4m_{ir}^2}, \tag{1}$$

$$S = 16\pi m_{ir}^2, \tag{2}$$

$$\delta S = 32\pi m_{ir}\delta m_{ir} \geq 0. \tag{3}$$

2 The discovery of Gamma Ray Bursts (GRBs)

A fundamental contribution was achieved by the advent of the gamma-ray astronomy that discovered in 1972, via the Vela satellites, the Gamma Ray Bursts (GRBs). The observations further evolved by one of the largest space missions, the Compton Gamma Ray Observatory (CGRO) with its BATSE and Egret Telescopes, which promoted the largest confrontation between the local (galactic) versus cosmological (extragalactic) nature of GRBs. An early model assuming a jetted emission from a rotating BH was there advanced to explain the observed gamma-ray emission of GRBs (see reviews of Rees & Mészáros (1992), Mészáros (2002), and Piran (2004)).

3 The Beppo-SAX GRBs era

A new "era" was initiated by the Italian–Dutch telescope Beppo-SAX, which associated in a single mission the expertise of the X-rays astronomers and the gamma-ray

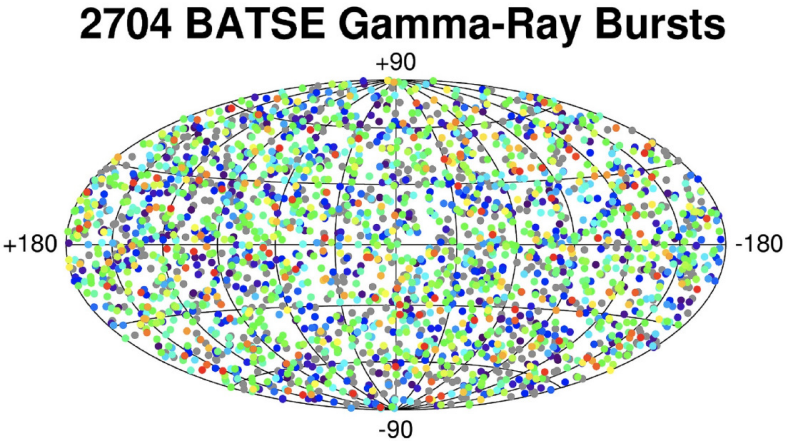


Figure 3 The homogeneous distribution of 2700 GRBs. Fluence is a measure of the total energy emitted in the burst. (Credit: CGRO BATSE Team.)

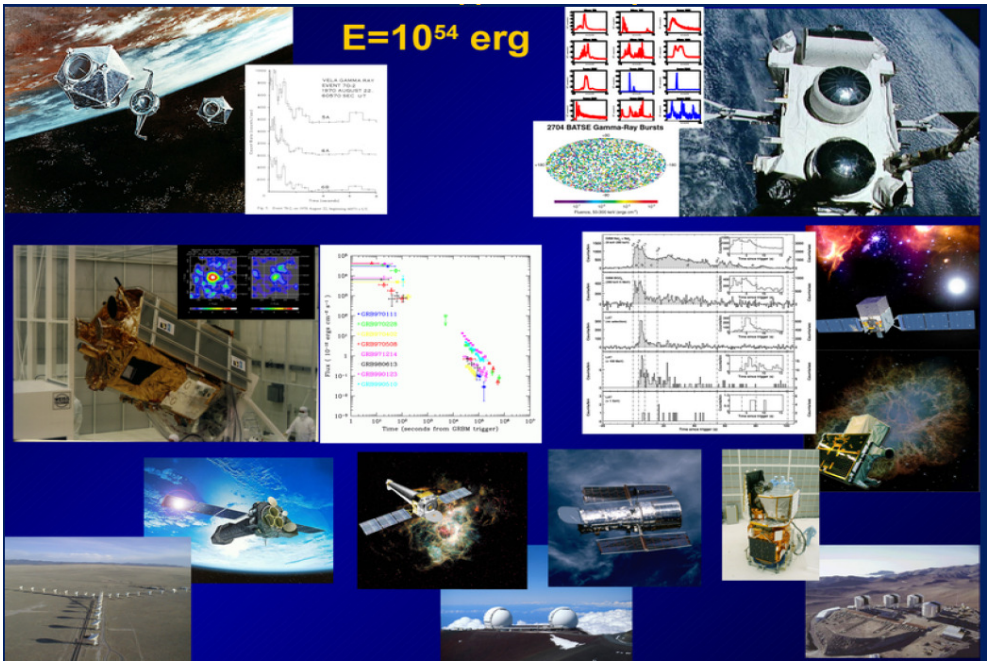


Figure 4 The launch of Beppo-SAX on April 30, 1996. From ICRANet archive.

astronomers, further extended to the extragalactic as well to the galactic optical communities, which allowed us to reach three main discoveries:

1. the improved GRBs localization of GRBs sources, using the X-ray afterglow, a new fundamental component of GRB description discovered by Beppo-SAX;

2. the firm determination of the GRB cosmological origin, from the measurement of their distance using their cosmological redshift (Metzger et al., 1997) and the consequent determination of their energetics of the order of 10^{54} ergs for GRB 970228 (Costa et al., 1997), observed by Beppo-SAX;
3. the temporal and spatial coincidence of GRBs with Type Ic SNe of energy 1049 erg in GRB980425A SN 1998BW (Galama et al., 1998).

4 The multi messenger era of GRBs

Following the Beppo-SAX mission, the exponential growth of observatories in all wavelengths, ranging from radio, optical, all the way to X-ray, Mev, Gev, Tev radiation, a prolific exponential growth of data followed in the recent 25 years.

Based on these data, the BDHN model was started by the concept of induced gravitational collapse (Rueda, Ruffini 1972), evolved collaboration with Los Alamos National Laboratory and Chris Fryer. The binary model assumes, as a progenitor, a binary system composed of a CO core and a binary NS companion (see Fig. 5). Three different BDHN types exist, mainly as a function of their binary period. The collapse of the CO core leads to the SN explosion with the creation of a νNS (pulsar), which originates the X-ray afterglow.

The main results:

1. the SN associated with the long GRBs, as soon as al relativistic effects are taken into account, have a common peak luminosity and time of occurrence of the peak as measured from the GRB trigger (details in Aimuratov et al., in preparation);
2. three different types of BdHN exist: BdhN I, with energies ranging from 10^{52} to 10^{54} and binary periods of minutes (an example is given in GRB 190114C, see Fig. 9); BDHN II from 10^{50} to 10^{52} with binary periods of hours (an example is given in GRB 190829A, see Wang, Rueda, et al. (2022); BdHN III from 10^{47} to 10^{50} (the example is given in GRB 171205 A, see Wang, Becerra, Fryer, Rueda, and Ruffini (2022));
3. the entire dynamics of GRBs are reduced to three contributions: 1) the SN explosion; 2) the SN ejecta accreting on the binary NS companion, leading to the formation of the BH in BdHN I and to the prompt emission in BDHN II; and 3) the SN ejecta, accreting on the νNS. The X-ray afterglow, present in all BDHN types, necessarily originates from the νNS by its synchrotron emission.

5 The paradigm change from “dead” to “alive” Black Hole

The detailed description of the new physics explains the entire energetics of GRBs as originating from classical and quantum electrodynamical processes, which substantially modify the initial assumptions of the gravitating particles characterizing a “dead Black Hole”, indicated in the early introduction of the BH in 1971. This has evolved in favour of the concept of “alive Black Hole”, whose first seed was planted

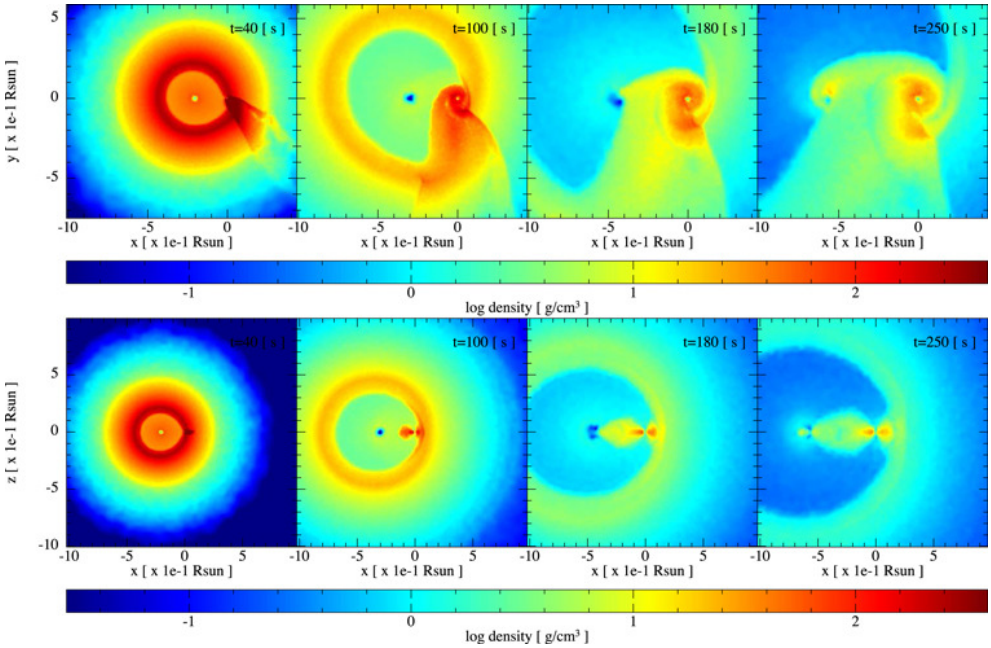


Figure 5 Snapshots of the SPH simulation of the IGC scenario presented in Becerra et al. (2019), here reproduced by kind permission. The initial binary system is formed by a CO_{core}, whose progenitor is a $M_{zams} = 25\,M_\odot$, and a $2\,M_\odot$ NS with an initial orbital period of approximately 5 min (Model 25M1p1e of Becerra et al. (2019)). The upper panel shows the mass density on the binary equatorial plane, at different simulation times, while the lower panel corresponds to the plane orthogonal to the binary equatorial plane. The reference system was rotated and translated in a way that the x-axis is along the line that joins the binary stars and the origin of the reference system is at the NS position. At $t = 40$ seconds (first frame from left to right), it can be seen that the particles captured by the NS have formed a kind of tail behind it, then these particles start to circularize around the NS, and a kind of thick disk is observed at $t = 100$ s (second frame from left to right). The material captured by the gravitational field of the NS companion is also attracted by the νNS and starts to be accreted by it as can be seen at $t = 180$ s (third frame). After around one initial orbital period, at $t = 250$ s, both stars have formed a kind of disk structure. The νNS is along the x-axis at: -2.02, -2.92, -3.73 and -5.64 for $t = 40$, 100, 180 and 250 s, respectively.

in our initial article by introducing the mass energy formula of the BH. The essential conceptual step in the evolution of the BH description has been the introduction of the concept of an "effective charge" function of the BH spin and the Wald magnetic field. Starting from these results we can as well pose new problems to be addressed:

1. the possible nature of SN 10^{54} as a GRB;
2. the universality of the X-ray afterglow in all long GRBs originating from the νNS pulsar;
3. the understanding of the supernova explosion, including the formation of the νNS pulsar.

				This Study			Literature		
GRB Name	SN Name	SN Type	z Redshift	$E_{\rm iso,\gamma}$ (erg)	$L_{\rm p,SN}$ ($\times 10^{42}$ erg s^{-1})	$t_{\rm p,SN}$ (days)	$E_{\rm iso,\gamma}$ ($\times 10^{52}$ erg)	$L_{\rm p,SN}$ ($\times 10^{42}$ erg s^{-1})	$t_{\rm p,SN}$ ($\times 10^{6}$ s)
980425	1998bw	Ic-BL	0.0085	$(8.6 \pm 0.2) \times 10^{47}$	7.33	15.16	0.000086	14.5	1.30464
011121	2001ke	Ic	0.362	$(7.8 \pm 2.1) \times 10^{52}$	5.90	17	7.8	$\sim 5.9, 13.7$	1.4688
021211	2002lt	Ic	1.006	$(1.12 \pm 0.13) \times 10^{52}$	7.20	14.00	0.828	–	2.16
030329	2003dh	Ic	0.1687	$(1.5 \pm 0.3) \times 10^{52}$	10.1	12.75	1, 515	10.1	1.1016
031203	2003lw	Ic	0.1055	$(8.6 \pm 4.0) \times 10^{49}$	12.6	17.33	0.0098	12.6	1.497312
050525	2005nc	Ic	0.606	$(2.5 \pm 0.43) \times 10^{52}$	4.47	13.10	2.945	–	–
060218	2006aj	Ic-BL	0.0334	$(5.3 \pm 0.3) \times 10^{49}$	6.47	10.42	0.0053	6.47	0.90029
081007A	2008hw	Ic	0.5295	$(1.5 \pm 0.4) \times 10^{51}$	14.0	12.00	0.15	~ 14	~ 1.0368
091127	2009nz	Ic	0.4904	$(1.5 \pm 0.2) \times 10^{52}$	12.0	15.00	1.5	~ 12	~ 1.296
100316D	2010bh	Ic-BL	0.0592	$> 5.9 \times 10^{49}$	5.67	8.76	> 0.0059	5.67	0.756864
101219B	2010ma	Ic	0.5519	$(4.2 \pm 0.5) \times 10^{51}$	15.0	11.80	0.42	15	1.01952
111209A	2011kl	SLSN-I	0.677	$(5.82 \pm 0.73) \times 10^{53}$	29.1	14.80	58.2	29.1	1.27872
120422A	2012bz	Ib/c	0.2825	$(2.4 \pm 0.8) \times 10^{50}$	14.8	14.45	0.024	14.8	1.24848
120714B	2012eb	Ib/c	0.3984	$(5.94 \pm 1.95) \times 10^{50}$	6.20	13.60	0.3174195	–	13.6 ± 0.7
130215A	2013ez	Ic	0.597				3.1	–	–
130427A	2013cq	Ic	0.3399	$(8.1 \pm 0.8) \times 10^{53}$	9.12	12.68	89	–	–
130702A	2013dx	Ic-BL	0.145	$(6.4 \pm 1.3) \times 10^{50}$	10.8	12.94	0.064	10.8, 19.2	1.118016
130831A	2013fu	Ib/c	0.4791	$(4.6 \pm 0.2) \times 10^{51}$	6.90	11.90	0.59221795	–	1.60704 ± 0.05789
161219B	2016jca	Ic-BL	0.1475	$(8.50 \pm 8.46) \times 10^{49}$	4.90	10.70	0.0858	10.4	0.92448
171010A	2017htp	Ic-BL	0.33	$(1.80 \pm 0.30) \times 10^{53}$	8.4	12.80	18, 22	21 ± 9	–
171205A	2017iuk	Ic-BL	0.0368	$(5.72 \pm 0.80) \times 10^{49}$	6.5	15.08	0.00218	–	1.09728
180728A	2018fip	Ic-BL	0.117	$(2.30 \pm 0.10) \times 10^{51}$	5.8	12.70	0.2545	–	1.27008 ± 0.25056
190114C	2019jrj	Ic	0.4245	$(3.0 \pm 0.5) \times 10^{53}$	6.0	10.50	30	–	1.62432 ± 0.31968
190829A	2019oyw	Ic-BL	0.0785	$(2.0 \pm 0.3) \times 10^{50}$	6.27	18.00	0.018	–	0.794016 ± 0.0216

Figure 6 Reproduced from Aimuratov at al. (in preparation) with their kind permission. Information on SN type is retrieved from Transient Name Server (www.wis-tns.org) and SIMBAD Astronomical Database (http://simbad.cds.unistra.fr/simbad/), except for the following events: SN 2001ke: Bloom et al. (2002); SN 2009nz: Berger et al. (2011); SN 2011kl: Greiner et al. (2015); SN 2019jrj: Melandri et al. (2022); SN 2019oyw: Hu et al. (2021). **References for** z: 980425: Galama et al. (1998); 011121: Infante et al. (2001); 021211: Vreeswijk et al. (2003); 030329: Thöne et al. (2007); 031203: Prochaska et al. (2003); 050525: Della Valle et al. (2006); 060218: Pian et al. (2006); 081007A: Berger et al. (2008); 091127: Vergani et al. (2011); 100316D: Bufano et al. (2012); 101219B: Sparre et al. (2011); 111209A: Vreeswijk et al. (2011); 120422A: Schulze et al. (2014); 120714B: Fynbo et al. (2012); 130215A: Cucchiara and Perley (2013); 130427A: Flores et al. (2013); 130702A: Mulchaey et al. (2013); 130831A: Cucchiara and Perley (2013); 161219B: Tanvir et al. (2016); 171010A: Kankare et al. (2017); 171205A: Izzo et al. (2017).

6 Conclusions

1. Having finally identified the process of formation of an "alive Black Hole";
2. we confirm that the mathematical structure of the "alive Black Hole" firmly follows the Kerr solution; and
3. the physics is dominated by the Christodoulou–Ruffini–Hawking mass energy formula and the leading terms of energy extraction stand on classical and quantum electrodynamics process.

7 Discussion

The ten basic principles of the Black Hole energy extraction:

1. The Black Hole is characterized by a Kerr solution;

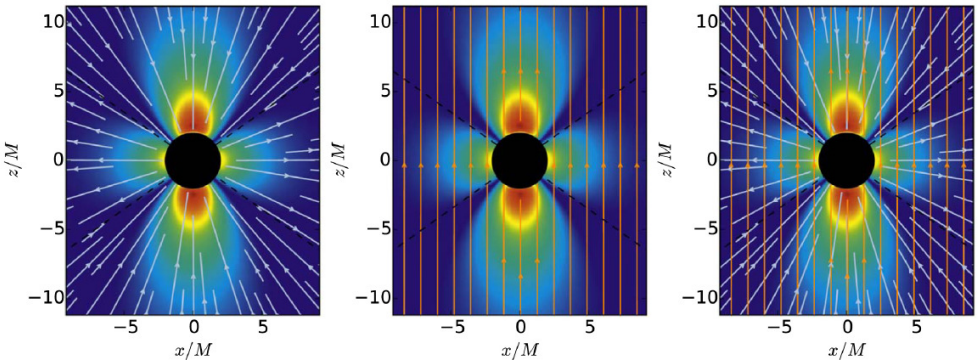


Figure 7 Reproduced from Rueda et al. (2022) with their kind permission. Electromagnetic field configuration for a *polar electronic jet*. Left: Electric field lines (blue-colored lines) of the Papapetrou–Wald solution for a BH spin parameter $a/M = 0.3$, in the xz plane in Kerr–Schild coordinates. Center: magnetic field lines (gold-colored lines). Right: Electric and magnetic field lines together. It can be directly checked from the slow-rotation expressions of the fields that the electric field intensity decreases from the polar axis to the equator along a contour of constant radial distance. The magnetic field is asymptotically (at infinity) parallel to the BH spin. The colored background is a density plot of the electric field energy density which decreases from red to blue. The BH horizon is represented by the black filled disk. Distances are in units of M and the fields in units of B_0. Electron acceleration (outward photon emission) occurs in the region where the electric field is inwardly directed. This region, limited by the dashed-black lines, is defined in the northern hemisphere by the spherical polar angles (measured clockwise from the rotation axis) $-\theta_\pm < \theta < \theta_\pm$, and by equatorial symmetry, in the southern hemisphere by $\pi - \theta_\pm < \theta < \pi + \theta_\pm$. At the angle $\theta_\pm$, the electric field reverses direction, i.e. $\vec{E} \cdot \vec{B} = 0$. For the above parameters, $\theta_\pm \approx 55°$. We have used the general transformation from Boyer–Lindquist to Kerr–Schild coordinates.

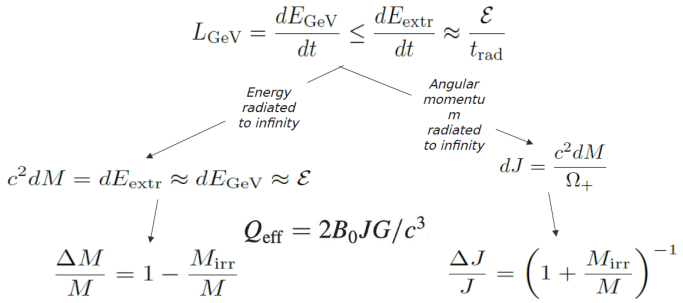


Figure 8 Reproduced from Rueda et al. (2022) with their kind permission.

2. That gravitating particle orbits in vacuum are of no physical nor astrophysical interest in GRBs;
3. That only nonstationary Kerr solutions can be of interest as astrophysical energy sources;
4. That energy extraction process necessarily fulfill the Irreducible Mass constraint;

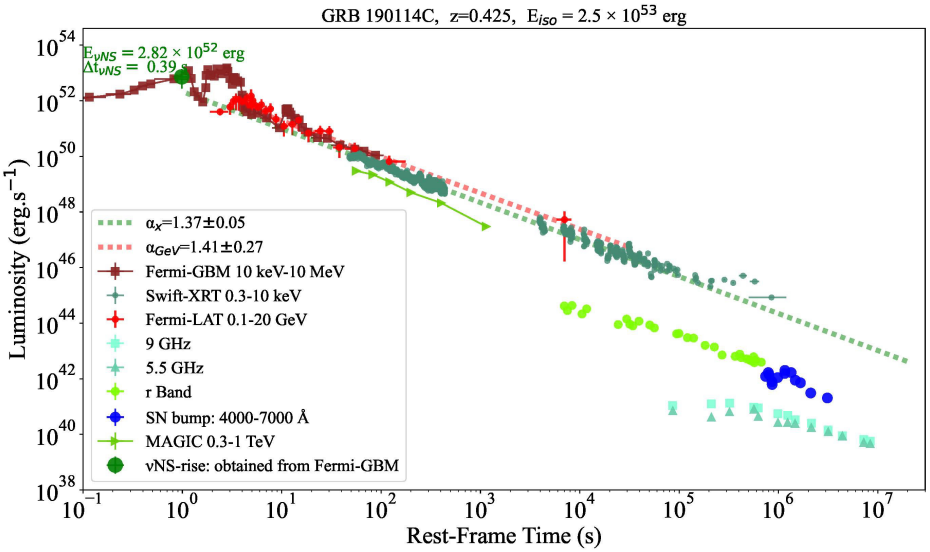


Figure 9 BdHNe I: GRB 190114C. Luminosity light-curves obtained from *Fermi*-GBM, in 10 keV–10 MeV, *Fermi*-LAT in 0.1 GeV–10 GeV, *Swift*-BAT in 15 keV–50 keV, *Swift*-XRT in 3 keV–10 keV and optical R band. The late X-ray afterglow luminosity of BdHN I GRB 190114C observed by *Swift*-XRT is best fit by a temporal decaying power law of $L_{\rm X} = (2.5 \pm 0.4) \times 10^{53}\ t^{1.44\pm0.01}$ erg s^{-1}. The light-curve of *Fermi*-LAT is fitted by temporal decaying power law of $L_{\rm GeV} = (4.6 \pm 2.9) \times 10^{53}\ t^{-1.94\pm0.04}$ erg. The prediction of the associated supernova by Ruffini, Moradi, et al. (2019) has been successfully observed by Melandri et al. (2019) has made GRB 190114C as a proper BdHN (Moradi et al., 2021b) to study the properties of GRB–SN sources. The rest-frame visual absolute magnitude of the SN associated with GRB 190114C is $\sim$ –18 mag (Melandri et al., 2019), which is $\sim$ 1 mag less than the famous SN 1998bw (Patat et al., 2001). This fainter brightness can be due to the extinction for this event (Kann et al., 2019). (Reproduced from Aimuratov at al., in preparation, with their kind permission.)

5. That non vacuum Kerr solutions with a uniform magnetic test field B_0 on the rotational axis can introduce an "effective charge" function of the BH spin and B_0;
6. That such an "effective" Kerr–Newman solution, embedded in a fully ionized plasma, can lead to energy extraction;
7. The energy extraction is only a function of the black hole spin; the magnitude of the background magnetic field B_0 remains constant, see Fig. 7;
8. The "effective charge" determines the black hole "inner engine" and the equation of motion of the plasma, see Fig. 8;
9. That the energy extraction process occurs in terms of quanta, see Fig. 8;
10. The process of energy extraction is repetitive and each energy extraction process gives origin to a new process, starting from a smaller value of the spin DJ and rotational energy $DE_{\rm rot}$, being B_0 constant.

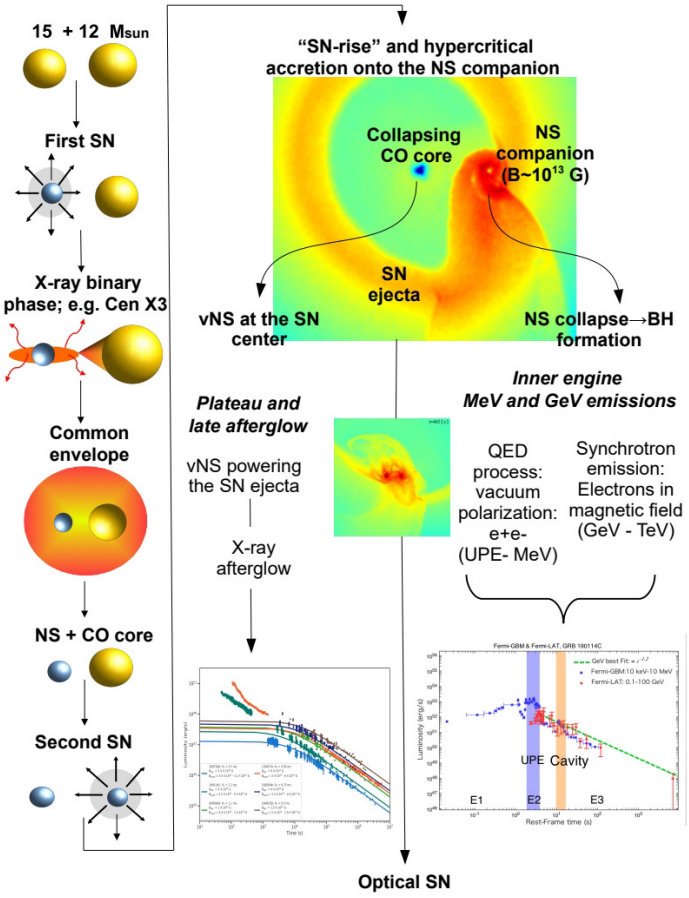


Figure 10 Schematic evolutionary path of a massive binary up to the emission of a BdHN. (a) Binary system composed of two main-sequence stars of 15 and 12 solar masses, respectively. (b) At a given time, the more massive star undergoes the core-collapse SN and forms an NS (which might have a magnetic field $B \sim 10^{13}$ G). (c) The system enters the X-ray binary phase. (d) The core of the remaining evolved star, rich in carbon and oxygen, for short CO_{core}, is left exposed since the hydrogen and helium envelope have been stripped by binary interactions and possibly multiple common-envelope phases (not shown in this diagram). The system is, at this stage, a CO_{core}–NS binary, which is taken as the initial configuration of the BdHN model (see, e.g., Becerra et al., 2019). (e) The CO_{core} explodes as SN when the binary period is of the order of few minutes, the SN ejecta of a few solar masses start to expand and a fast rotating, newborn NS, for short νNS, is left in the center. (f) The SN ejecta accrete onto the NS companion, forming a massive NS (BdHN II) or a BH (BdHN I; this example), depending on the initial NS mass and the binary separation. Conservation of magnetic flux and possibly additional MHD processes amplify the magnetic field from the NS value to $B \sim 10^{14}$ G around the newborn BH. At this stage the system is a νNS–BH binary surrounded by ionized matter of the expanding ejecta. (g) The accretion, the formation and the activities of the BH contribute to the GRB prompt gamma-ray emission and GeV emission. See details in Rueda et al. (2020).

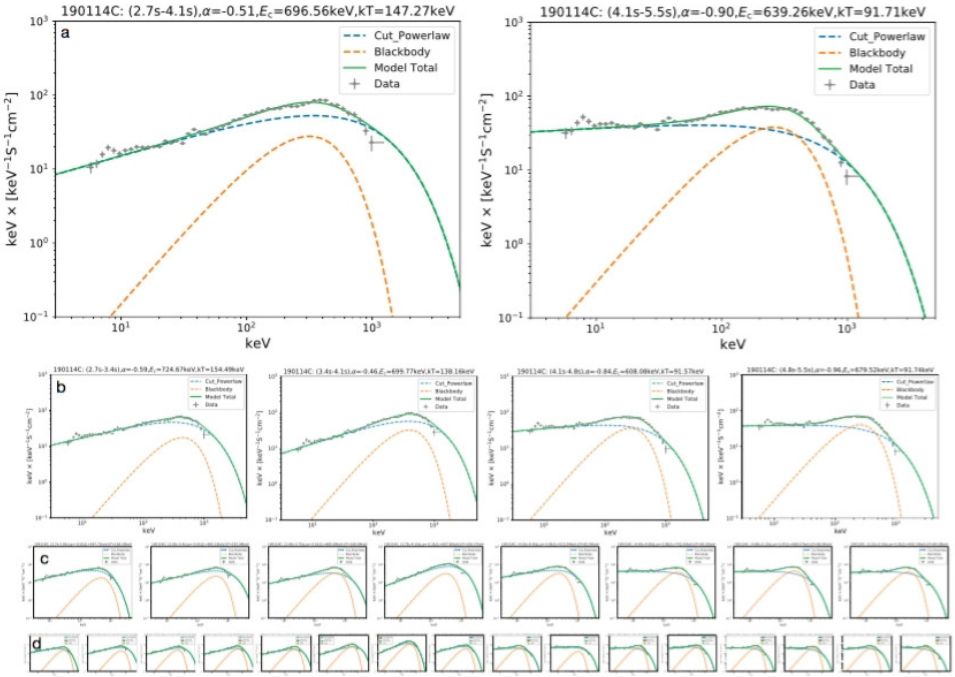


Figure 11 Time-resolved spectral analysis of UPE phase GRB 190114C: from $t = 2.7$ s ($t_{\rm rf} = 1.9$ s) to $t = 5.5$ s ($t_{\rm rf} = 3.9$ s). The time interval is divided into (a) two parts; (b) four parts; (c) eight parts, and (d) sixteen parts. Plots are taken from Ruffini, Li, et al. (2019) with permission of authors.

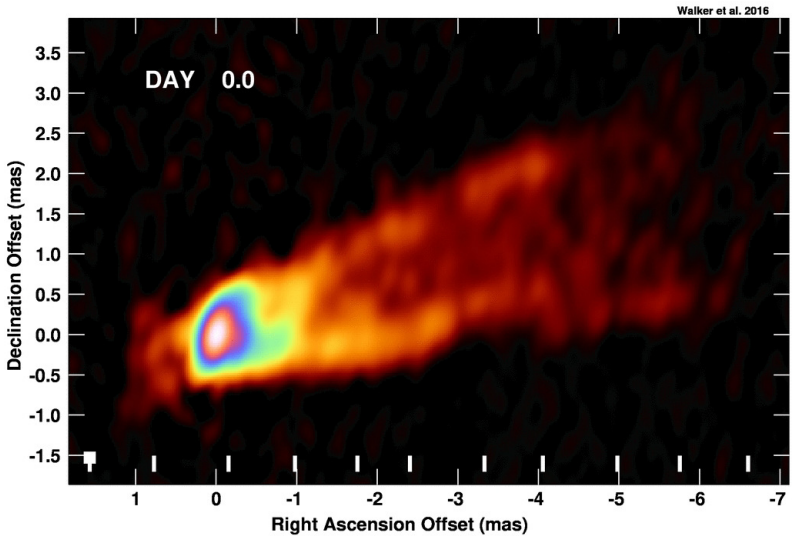


Figure 12 The astrophysical properties of the *inner engine* for M87* is similar to GRB 190114C. The timescale of the emission in GRBs is too short to be probed directly by current observational facilities. Direct evidence of the value and discreteness might come out instead from the observation of large BHs. For example in the case of M87*, for fiducial parameters $M = 6 \times 10^9\ M_\odot$, $\alpha = 0.1$, and $B_0 = 10\ G$, the *inner engine* theory predicts a high-energy (GeV) emission with a luminosity of a few 10^{43} erg s^{-1}, with a timescale of up to tenths of seconds; see Moradi et al. (2021a); Rueda & Ruffini (2020).

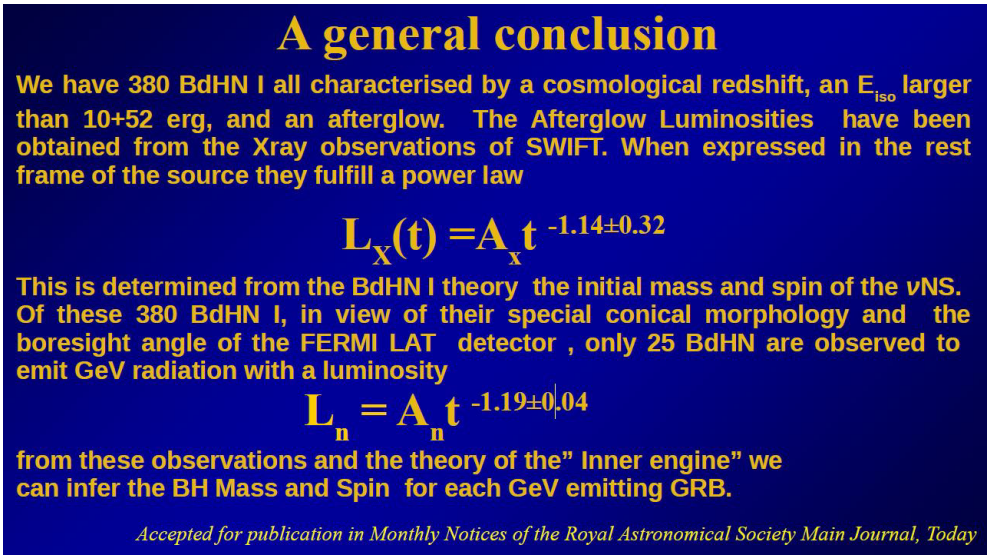


Figure 13

References

Aimuratov, Y., Becerra, L.M., Bianco, C.L. et al. (2023), in preparation.

Becerra, L., Ellinger, C.L., Fryer, C.L., Rueda, J.A., & Ruffini, R. (2019, January), ApJ, 871, 14.

Berger, E., Chornock, R., Holmes, T.R. et al. (2011, December), ApJ, 743(2), 204.

Berger, E., Fox, D.B., Cucchiara, A., & Cenko, S.B. (2008, January), GRB Coordinates Network, 8335, 1.

Bloom, J.S., Kulkarni, S.R., Price, P.A. et al. (2002, June), ApJ, 572(1), L45-L49.

Bufano, F., Pian, E., Sollerman, J. et al. (2012, July), ApJ, 753(1), 67.

Christodoulou, D. (1970, Nov), Phys. Rev. Lett., 25(22), 1596-1597.

Christodoulou, D., & Ruffini, R. (1971, December), Phys. Rev. D, 4, 3552-3555.

Costa, E., Frontera, F., Heise, J. et al. (1997, June), Nature, 387, 783.

Cucchiara, A., & Perley, D. (2013, January), GRB Coordinates Network, 15144, 1.

Della Valle, M., Malesani, D., Bloom, J.S. et al. (2006, May), ApJ, 642(2), L103-L106.

Flores, H., Covino, S., Xu, D. et al. (2013, January), GRB Coordinates Network, 14491, 1.

Fynbo, J.P.U., de Ugarte Postigo, A., D'Elia, V., Xu, D., & Malesani, D. (2012, January), GRB Coordinates Network, 13477, 1.

Galama, T.J., Vreeswijk, P.M., van Paradijs, J. et al. (1998, October), Nature, 395(6703), 670-672.

Greiner, J., Mazzali, P.A., Kann, D.A. et al. (2015, July), Nature, 523(7559), 189-192.

Hawking, S.W. (1971, May), Phys. Rev. Lett., 26(21), 1344-1346.

Hawking, S.W. (1972, June), Communications in Mathematical Physics, 25(2), 152-166.

Hu, Y.D., Castro-Tirado, A.J., Kumar, A. et al. (2021, February), A&A, 646, A50.

Infante, L., Garnavich, P.M., Stanek, K.Z., & Wyrzykowski, L. (2001, January), GRB Coordinates Network, 1152, 1.

Izzo, L., Selsing, J., Japelj, J. et al. (2017, January), GRB Coordinates Network, 22180, 1.

Kankare, E., O'Neill, D., Izzo, L. et al. (2017, January), GRB Coordinates Network, 22002, 1-2018.

Kann, D.A., Thoene, C.C., Selsing, J. et al. (2019, January), GRB Coordinates Network, 23710, 1.

Landau, L.D., & Lifshitz, E.M. 1975, The classical theory of fields. Course of theoretical physics – Pergamon International Library of Science, Technology, Engineering and Social Studies, Oxford: Pergamon Press, 4th rev. Engl. ed.

Melandri, A., Izzo, L., D'Avanzo, P. et al. (2019, January), GRB Coordinates Network, 23983, 1.

Melandri, A., Izzo, L., Pian, E. et al. (2022, March), A&A, 659, A39.

Mészáros, P. (2002), ARA&A, 40, 137.

Metzger, M. R., Djorgovski, S. G., Kulkarni, S. R. et al. (1997, June), Nature, 387, 878-880.

Moradi, R., Rueda, J. A., Ruffini, R., & Wang, Y. (2021a, May), A&A, 649, A75.

Moradi, R., Rueda, J. A., Ruffini, R., & Wang, Y. (2021b, November), A&A.

Mulchaey, J., Kasliwal, M. M., Arcavi, I., Bellm, E., & Kelson, D. (2013, July), The Astronomer's Telegram, 5191, 1.

Patat, F., Cappellaro, E., Danziger, J. et al. (2001, July), ApJ, 555(2), 900-917.
Pian, E., Mazzali, P.A., Masetti, N. et al. (2006, August), Nature, 442(7106), 1011-1013.
Piran, T. (2004, October), Reviews of Modern Physics, 76, 1143- 1210.
Prochaska, J.X., Bloom, J.S., Chen, H.W., Hurley, K., Dressler, A., & Osip, D. (2003, January), GRB Coordinates Network, 2482, 1.
Rees, M.J., & Meszaros, P. (1992, September), MNRAS, 258, 41P- 43P.
Rueda, J.A., & Ruffini, R. (2020, April), European Physical Journal C, 80(4), 300.
Rueda, J.A., Ruffini, R., Karlica, M., Moradi, R., & Wang, Y. (2020, April), ApJ, 893(2), 148.
Rueda, J.A., Ruffini, R., & Kerr, R.P. (2022, April), ApJ, 929(1), 56.
Ruffini, R., Li, L., Moradi, R. et al. (2019, April), arXiv e-prints.
Ruffini, R., Moradi, R., Aimuratov, Y. et al. (2019, January), GRB Coordinates Network, 23715, 1.
Ruffini, R., & Wheeler, J.A. (1971, January), Physics Today, 24(1), 30.
Schulze, S., Malesani, D., Cucchiara, A. et al. (2014, June), A&A, 566, A102.
Sparre, M., Sollerman, J., Fynbo, J.P.U. et al. (2011, July), ApJ, 735(1), L24.
Tanvir, N.R., Kruehler, T., Wiersema, K., Xu, D., Malesani, D., Milvang-Jensen, B., & Fynbo, J.P.U. (2016, January), GRB Coordinates Network, 20321, 1.
Thöne, C.C., Greiner, J., Savaglio, S., & Jehin, E. (2007, December), ApJ, 671(1), 628-636.
Vergani, S.D., Flores, H., Covino, S. et al. (2011, November), A&A, 535, A127.
Vreeswijk, P., Fruchter, A., Hjorth, J., & Kouveliotou, C. (2003, January), GRB Coordinates Network, 1785, 1.
Vreeswijk, P., Fynbo, J., & Melandri, A. (2011, January), GRB Coordinates Network, 12648, 1.
Wang, Y., Becerra, L.M., Fryer, C.L., Rueda, J.A., & Ruffini, R. (2022, August), arXiv e-prints, arXiv:2208.02725.
Wang, Y., Rueda, J.A., Ruffini, R. et al. (2022, September), ApJ, 936(2), 190.